Supplemental Material (not copyedited or formatted) for: Justin D. Yeakel, Mason Fan, Emily Jane McTavish, Anna Carolina de Almeida, Christopher P. Kempes, Luís M. A. Bettencourt, Sora Kim, Greg Breed. 2026. "An Origin for the Allometric Scaling of Mammalian Fat Reflects Populations Living on the Edge." The American Naturalist 208(5). DOI: https://doi.org/10.1086/742753.

Supplementary Appendices:

An origin for the allometric scaling of mammalian fat reflects populations living on the edge

Justin D. Yeakel[1,2,*], Mason Fan[1], Emily Jane McTavish[1], Anna Carolina de Almeida[1], Christopher P. Kempes[2], Luís M. A. Bettencourt[2,3], Sora Kim[1], Greg Breed[4]

1. Life & Environmental Sciences, University of California Merced, Merced, California, USA;
2. The Santa Fe Institute, Santa Fe, New Mexico, USA;
3. University of Chicago, Chicago, Illinois, USA;
4. University of Alaska, Fairbanks, Alaska, USA;

∗ Corresponding author; e-mail: jyeakel@ucmerced.edu.

Manuscript elements: figures 1-5 table 1, Supplement Appendices S1-S4.

Keywords: Allometric scaling; Fat reserves; Foraging energetics; Starvation; Fasting endurance.

Manuscript type: Article.

Prepared using the suggested LaTeX template for *Am. Nat.*

Supplemental Material (not copyedited or formatted) for: Justin D. Yeakel, Mason Fan, Emily Jane McTavish, Anna Carolina de Almeida, Christopher P. Kempes, Luís M. A. Bettencourt, Sora Kim, Greg Breed. 2026. "An Origin for the Allometric Scaling of Mammalian Fat Reflects Populations Living on the Edge." The American Naturalist 208(5). DOI: https://doi.org/10.1086/742753.

Supplementary Appendices

S1 Empirical datasets

Empirical data documenting fat mass M_f as a function of body mass M were gathered from seven primary sources (George et al., 2007; Lund et al., 2025; Navarrete et al., 2011; Pitts and Bullard, 1968; Pond, 1978; Pond and Mattacks, 1985; Ryg et al., 1993). Collectively, these datasets capture mammalian species spanning roughly the known body size range for mammals – from the masked shrew (*Sorex cinereus*) at 0.004 kg to the fin whale (*Balaenoptera physalus*) at 89×10^5 kg – and include altogether 57 families. Some datasets are biased towards specific groups of organisms; for example, Navarrete et al. (2011) primarily include smaller mammals such as rodents, primates, and carnivorans, with the largest-bodied species a 70 kg captive tiger, with wild species dominating the smaller size classes and captive species dominating the larger size classes. Others, such as those collected from the American Offshore Whaling Logbook (Lund et al., 2025), include only cetaceans.

Range	Model	Term	Est.	Std. Error	n_{obs}
All M	OLS	a	-2.750	0.065	218
		b	1.134	0.015	
All M	PGLS	a	-3.068	1.966	158
		b	1.145	0.052	
$M > 0.5$ kg	OLS	a	-2.926	0.110	138
		b	**1.171**	0.023	
$M > 0.5$ kg	PGLS	a	-3.087	1.654	97
		b	**1.139**	0.061	

Table S1: OLS (all species) and PGLS (taxonomically resolved subset) fits for $\log(M_f) = a + b \log M$ across all species and for the subset $M > 0.5$ kg. For large-bodied species the PGLS slope overlaps the OLS estimate. We adopt both the OLS slope of 1.17 and the PGLS slope of 1.14 for species with $M > 0.5$ kg (bold-faced) to bound subsequent analyses. All slope estimates are highly significant ($p \ll 0.001$).

Some cetacean data were collected from the American Offshore Whaling Logbook (Lund et al., 2025), which provide barrels of oil harvested from sperm whales (*Physeter macrocephalus*), right whales (*Eubalaena australis*), pilot whales (*Globicephala macrorhynchus*), and several others, and were converted to fat mass using the conversion described in George et al. (2007) from

Supplemental Material (not copyedited or formatted) for: Justin D. Yeakel, Mason Fan, Emily Jane McTavish, Anna Carolina de Almeida, Christopher P. Kempes, Luís M. A. Bettencourt, Sora Kim, Greg Breed. 2026. "An Origin for the Allometric Scaling of Mammalian Fat Reflects Populations Living on the Edge." The American Naturalist 208(5). DOI: https://doi.org/10.1086/742753.

bowhead whale individuals. This conversion is based on the ratio of blubber weight to total weight, at ca. 44%, meaning that fat mass derived from this conversion is by definition isometric. This conversion factor may also be inappropriate for some species that it is applied, such as orcas, likely to have a different mass-fat relationship than those of bowhead whales. These estimated data using the conversion factor (blue points, main text fig 2), while filling out missing size classes, were not included in the statistical analyses described in the paper and do not markedly change the mass-fat scaling relationship.

See Table. S1 for estimated OLS and PGLS fits referenced in the main text. See the archived Zenodo repository (`https://doi.org/10.5281/zenodo.17280285`) for supplementary data and code used in the analyses.

S2 Foraging model

A Resource distributions

The resource landscape is set by *i*) the resource density μ [g m^{-3}], *ii*) the dispersion parameter $\alpha = 4$, *iii*) the patchiness exponent ζ, and *iv*) the resource energy denstiy δ [kJ/g] (Table S2). As described in the main text, resources are converted to a bite-density field as $q = \mu/\beta$, where $\beta = \beta_0 M^{\beta_1}$ [g bite^{-1}] represents the herbivore's bite size (Shipley et al., 1994).

We assume the focal herbivore must share the resources contained in its 'instantaneous' reaction cross-section, a body-size-dependent window of width w and height h, with a local competitor load $n = d/(wh)$ [inds m^{-2}], where d is the number of conspecifics expected to interact within the broader daily foraging corridor, defining the sampling area. The reaction cross-section defines the vertical surface where the herbivore forager interacts with the volumetric resource environment in which it is foraging, where $w = w_0 M^{w_1}$ [m] represents the horizontal reaction distance (cf. Pawar et al., 2012), and $h = h_0 M^{h_1}$ [m] represents the vertical shoulder height of the forager (Larramendi, 2015).

The number of competitors is defined as $d = 1 + pa_c$, where p is the population density of

Supplemental Material (not copyedited or formatted) for: Justin D. Yeakel, Mason Fan, Emily Jane McTavish, Anna Carolina de Almeida, Christopher P. Kempes, Luís M. A. Bettencourt, Sora Kim, Greg Breed. 2026. "An Origin for the Allometric Scaling of Mammalian Fat Reflects Populations Living on the Edge." The American Naturalist 208(5). DOI: https://doi.org/10.1086/742753.

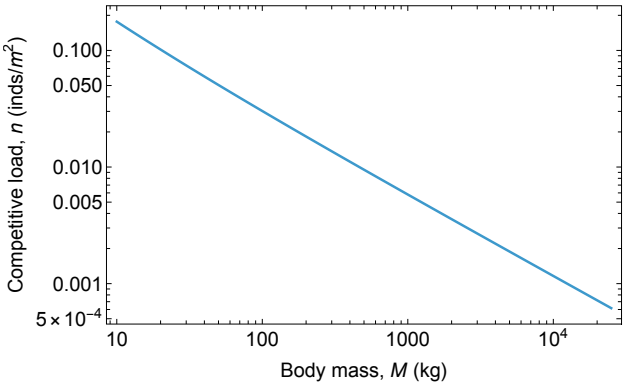


Figure S1: Competitive load n as a function of herbivore body mass M.

conspecifics following the Damuth relationship (Damuth, 1987), where $p = p_0 M^{p_1}$ [inds m^{-2}], a_c [m^2] is the maximum area foraged within a daily traveled corridor, and the '1' accounts for the focal individual. The foraging corridor is calculated as the distance a forager is capable of traveling in a daily foraging bout multiplied by a lateral width of 2 meters, such that $a_c = 2vt_{\text{bout}}$, where v is the forager's velocity [m s^{-1}] (Kramer and Prins, 2010) and t_{bout} is the expected temporal duration of the foraging bout (Owen-Smith, 1988), where $t_{\text{bout}} = tb_0 M^{tb_1}$ (Table S3). We note that the lateral width of 2 meters defining the foraging corridor establishes the day-long foraging trajectories of the potential competition load and is distinct from the reaction cross-section. Together, this means that the competitive load n declines with larger herbivore body sizes (fig. S1).

Following spatial-partitioning frameworks (e.g., Bhat et al., 2020; Holland et al., 2009), competition rescales both the mean and variance of bite encounters as $q_{\text{ind}} = q/n$, and $\sigma^2_{\text{ind}} = q^2/(n^\zeta \alpha)$ (such that $\alpha_{\text{ind}} = \alpha n^{\zeta-2}$), respectively, where the exponent ζ modulates how much patchiness persists after resources are subdivided among conspecifics. To capture heterogeneity, we model the linear bite-encounter rate along the forager's path $\Lambda \sim \text{Gamma}(\alpha_{\text{ind}}, q_{\text{ind}}/\alpha_{\text{ind}})$, so that $\mathbb{E}\{\Lambda\} = q_{\text{ind}}$ and $\text{Var}\{\Lambda\} = q^2_{\text{ind}}/\alpha_{\text{ind}}$. The scaling of patchiness and size is thus determined by the exponent ζ, and its effect on the scaling of the resource distribution with body size can be

Supplemental Material (not copyedited or formatted) for: Justin D. Yeakel, Mason Fan, Emily Jane McTavish, Anna Carolina de Almeida, Christopher P. Kempes, Luís M. A. Bettencourt, Sora Kim, Greg Breed. 2026. "An Origin for the Allometric Scaling of Mammalian Fat Reflects Populations Living on the Edge." The American Naturalist 208(5). DOI: https://doi.org/10.1086/742753.

Parameter	Meaning	Units	Value(s)
μ	Resource density	$\mathrm{g}\cdot\mathrm{m}^{-3}$	var.
α	Resource dispersion	–	4
ζ	Patchiness exp.	–	(1,2.15)
δ	Energy density	$\mathrm{kJ}\cdot\mathrm{g}^{-1}$	18.2
β	Bite size	$\mathrm{g}\cdot\mathrm{bite}^{-1}$	$\beta_0 M^{\beta_1}$
β_0	Bite size const.	$(\mathrm{g}\cdot\mathrm{bite}^{-1})\cdot\mathrm{kg}^{-\beta_1}$	0.002
β_1	Bite size exp.	–	0.969
q	Resource bite density	$\mathrm{bites}\cdot\mathrm{m}^{-3}$	$\mu\beta^{-1}$
n	Local competitor load	$\mathrm{inds}\cdot\mathrm{m}^{-2}$	$d(wh)^{-1}$
w	Reaction distance	m	$w_0 M^{w_1}$
w_0	Reaction distance const.	$\mathrm{m}\cdot\mathrm{kg}^{-w_1}$	5.0
w_1	Reaction distance exp.	–	0.33
h	Reaction height	m	$h_0 M^{h_1}$
h_0	Reaction height const.	$\mathrm{m}\cdot\mathrm{kg}^{-h_1}$	0.15
h_1	Reaction height exp.	–	0.36
d	Number of competitors	inds	$1+p\cdot c$
p	Comp. density	$\mathrm{inds}\cdot\mathrm{m}^{-2}$	$p_0 M^{p_1}$
p_0	Comp. density const.	$(\mathrm{inds}\cdot\mathrm{m}^{-2})\cdot\mathrm{kg}^{-p_1}$	5.4×10^{-5}
p_1	Comp. density exp.	–	-0.77
a_c	Foraging corridor area	m^2	$2vt_{\mathrm{bout}}$
v	Herbivore velocity	$\mathrm{m}\cdot\mathrm{s}^{-1}$	$v_0 M^{v_1}$
v_0	Herbivore velocity const.	$(\mathrm{m}\cdot\mathrm{s}^{-1})\cdot\mathrm{kg}^{-v_1}$	0.5
v_1	Herbivore velocity exp.	–	0.13

Table S2: Resource distribution parameters, definitions, units, and values.

observed by evaluating the coefficient of variation (CV), expressed as

$$\mathrm{CV}_{\mathrm{res}} = \frac{n^{1-\zeta/2}}{\sqrt{\alpha}}. \tag{S1}$$

Because the competitive load n varies with herbivore body mass, the $\mathrm{CV}_{\mathrm{res}}$ also varies with body mass, but does so differently for alternative values of ζ. As shown in fig. S2A, when $\zeta < 2$, $\mathrm{CV}_{\mathrm{res}}$ declines with increasing M; when $\zeta = 2$, $\mathrm{CV}_{\mathrm{res}}$ is invariant with respect to M; when $\zeta > 2$, $\mathrm{CV}_{\mathrm{res}}$ increases with increasing M. This allows us to examine the effects of alternative resource environments on herbivore foraging, as discussed in the main text.

Conditional on the linear bite-encounter rate Λ, the distance between resources is drawn from $D|\Lambda \sim \mathrm{Exponential}(\mathrm{rate} = \Lambda)$. This Gamma-Exponential mixture (a Lomax/Pareto-II distribution) captures the heavy-tailed spacing that arises when food patches are highly clumped. As the forager moves forward through its environment bite by bite, it samples a vertical cross-section of resources, sweeping out a rectangular cross-section through a three-dimensional volume (main text fig. 1). The expected distance between bites along the forager's path (bites/m) can then be

Supplemental Material (not copyedited or formatted) for: Justin D. Yeakel, Mason Fan, Emily Jane McTavish, Anna Carolina de Almeida, Christopher P. Kempes, Luís M. A. Bettencourt, Sora Kim, Greg Breed. 2026. "An Origin for the Allometric Scaling of Mammalian Fat Reflects Populations Living on the Edge." The American Naturalist 208(5). DOI: https://doi.org/10.1086/742753.

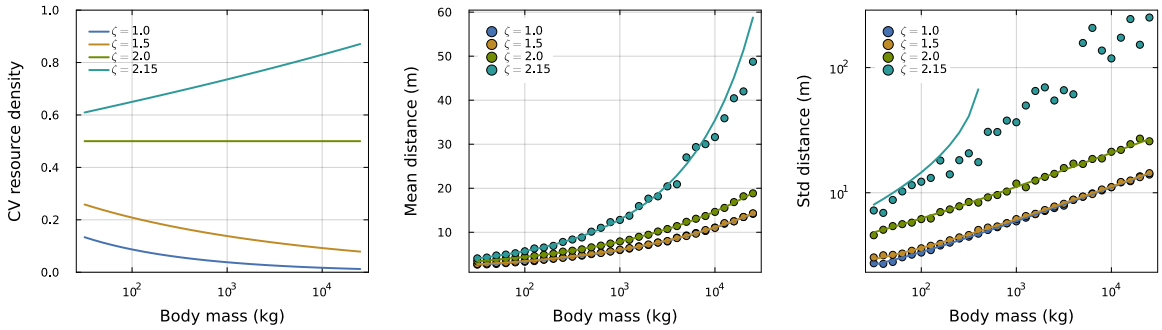


Figure S2: A. The experienced coefficient of variation for the resource density (see main text eq. 1) as a function of body mass M for different values of the patchiness exponent ζ. B. The expected (mean) distance between bites [m] (eq. S2) as a function of body mass M for different values of the patchiness exponent ζ. Lines represent analytical expectations; points represent simulated values. C. The standard deviation in distance between bites [m] (eq. S3) as a function of body mass M for different values of the patchiness exponent ζ. Lines represent analytical expectations; points represent simulated values. The analytical derivation for $\zeta = 2.15$ does not hold for large body masses.

expressed as

$$\mathbb{E}\{D = d\} = \frac{\alpha n^{\zeta-1}}{q(\alpha n^{\zeta-2} - 1)}, \tag{S2}$$

whereas the variance is given by

$$\mathrm{Var}\{D = d\} = \frac{(\alpha n^{\zeta-2})^3}{(q/n)^2(\alpha n^{\zeta-2} - 1)^2(\alpha n^{\zeta-2} - 2)}. \tag{S3}$$

The expected travel time between bites is then given by

$$\mathbb{E}\{T_{\text{travel}} = t_{\text{travel}}\} = \frac{1}{v}\frac{\alpha n^{\zeta-1}}{q(\alpha n^{\zeta-2} - 1)}. \tag{S4}$$

We observe that the travel time between bites is shorter in enriched environments and longer in poor environments (stippled versus solid lines, fig. S4). It is also clear that increasing patchiness (higher ζ) increases the expected travel time between bites (colored lines, fig. S4).

Supplemental Material (not copyedited or formatted) for: Justin D. Yeakel, Mason Fan, Emily Jane McTavish, Anna Carolina de Almeida, Christopher P. Kempes, Luís M. A. Bettencourt, Sora Kim, Greg Breed. 2026. "An Origin for the Allometric Scaling of Mammalian Fat Reflects Populations Living on the Edge." The American Naturalist 208(5). DOI: https://doi.org/10.1086/742753.

B Accumulation of gains and costs

Our minimal foraging model assumes that an herbivore of size M forages over the course of a day, accumulating energetic gain g from bites as well as metabolic costs c (Table S3). Time spent foraging consists of two events: *i*) travel time between bites (see discussion above), and *ii*) the time spent chewing at each bite. Time spent chewing is assumed to following the allometric relationship $t_{\text{chew}} = tc_0 M^{tc_1}$ [s]. The foraging bout ends when *i*) the expected bout time t_{bout} is reached, or if the herbivore reaches its gut capacity. Gut capacity follows the allometric scaling relationship $u = \delta u_0 M^{u_1}$ [kJ], but where the normalization constant u_0 and exponent u_1 differ for herbivores with different digestive anatomies (Müller et al., 2013). Note that while gut capacity is given is in grams of dry matter, we have converted it to kJ assuming the energy density δ. We assess the effects of four modes of herbivory – caecum-fermenting, hindgut-fermenting, non-rumen foregut-fermenting, and rumen foregut-fermenting – through their differential effect on gut capacity limiting the time spent foraging.

As herbivores forage, they accumulate gains (through bites) as well as metabolic costs. We assume a basal metabolic rate for the time spent chewing, and the time external to the foraging bout, where $B = B_0 M^{B_1}$, and a field metabolic rate for the travel time between bites $F = F_0 M^{F_1}$. In enriched environments, bites are numerous and the distance between them is small. In this case, these gut-limited foragers reach their gut capacity before the end of the foraging bout, with gains scaling in proportion to gut capacity (see fig. S3).

We calculate the gain surplus exponent γ, where $g_S \propto M^{\gamma}$ from daily simulations of foragers with body masses ranging from $M = 50$ to $M = 25000$ kg - roughly the size of a small gazelle to 1.5$\times$ the size estimates for the largest terrestrial mammalian herbivores, which include *Paraceratherium* and *Deinotherium* (Yeakel et al., 2018). For each value of environmental richness μ and patchiness ζ, and for each measured body mass M, gains and costs are assessed and averaged across replicates. The simulated gain surplus slope is measured across $\log(g_S)$ and $\log(M)$ for larger herbivores. For smaller herbivores, the slope of the gain surplus is highly nonlinear in

Supplemental Material (not copyedited or formatted) for: Justin D. Yeakel, Mason Fan, Emily Jane McTavish, Anna Carolina de Almeida, Christopher P. Kempes, Luís M. A. Bettencourt, Sora Kim, Greg Breed. 2026. "An Origin for the Allometric Scaling of Mammalian Fat Reflects Populations Living on the Edge." The American Naturalist 208(5). DOI: https://doi.org/10.1086/742753.

log-log space for reasons that will be discussed below. The measured gain surplus slope γ is then evaluated as a function of both environmental richness μ and for the different categories of herbivore fermentation (fig. S3).

C *Resource rich and resource poor environments*

When resources are plentiful, individual foragers are able to fill their gut prior to the end of a foraging bout (gut-limited environments). In such environments, the travel time between bites is short, allowing individuals to achieve high rates of gain at lower expense. In this case, we expect $g \approx \delta g^{\text{gut}}$, where g^{gut} is the herbivore's gut capacity [g], such that $g^{\text{gut}} = g_0^{\text{gut}} M^{g_1^{\text{gut}}}$, with different exponents for different fermentation pathways. In gut-limited environments, both simulation results and analytical approximations (squares and circles, respectively, fig. S3) of the gain surplus scaling converge. In this regime, the scaling of g_S is equivalent to gut capacity scaling as $M \to \infty$. For the mass range explored here, g_S has a slightly steeper relationship with body mass compared to gut capacity (vertical lines in fig. S3). Because herbivore gut capacities scale sublinearly with body mass, it is notable that the gain surplus in these environments is also sublinear, and not superlinear as one would expect from the observed mass-fat relationship.

When resources are scarce, the end of the foraging bout is reached before the herbivore's gut is filled (time-limited environments). In this case, the expected resource gain $\mathbb{E}\{G = g\}$ is given by

$$\mathbb{E}\{G = g\} = \delta\beta\mathbb{E}\{N_e\}, \tag{S5}$$

where $\mathbb{E}\{N_e\}$ is the expected number of bites encountered within the foraging bout, given by

$$\mathbb{E}\{N_e = n_e\} = \frac{t_{\text{bout}}}{\mathbb{E}\{T_{\text{travel}}\} + t_{\text{chew}}}, \tag{S6}$$

and as discussed above, $\mathbb{E}\{T_{\text{travel}}\}$ is given by eq. S4. Due to Jensen's inequality (Denny, 2017), $\mathbb{E}\{N_e\}$ must be viewed skeptically, and because $\text{Var}\{D\}$ (and by extension travel time) is on the same order as $\mathbb{E}\{D\}$ (fig. S2B,C), approximations such as the Delta Method (Hilborn and Mangel,

Supplemental Material (not copyedited or formatted) for: Justin D. Yeakel, Mason Fan, Emily Jane McTavish, Anna Carolina de Almeida, Christopher P. Kempes, Luís M. A. Bettencourt, Sora Kim, Greg Breed. 2026. "An Origin for the Allometric Scaling of Mammalian Fat Reflects Populations Living on the Edge." The American Naturalist 208(5). DOI: https://doi.org/10.1086/742753.

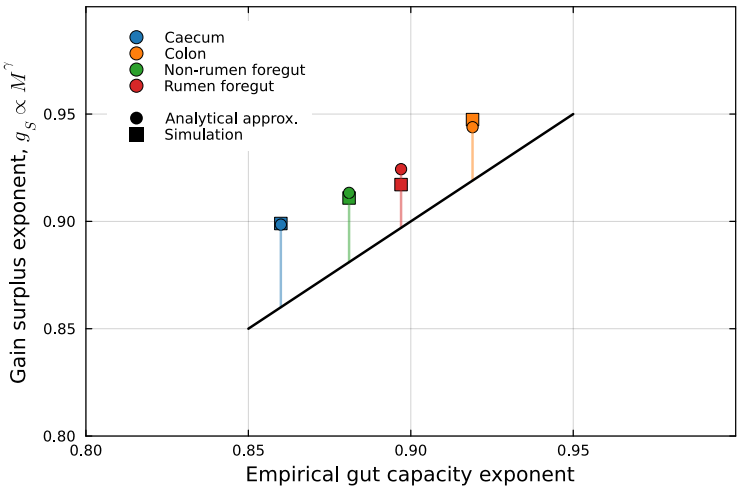


Figure S3: The gain surplus exponent γ in highly enriched environments (high μ) versus the gut capacity exponent (Müller et al., 2013) for different caecum, colon, non-rumen foregut, and rumen foregut fermenters. While the gain surplus is in all cases a steeper relationship across body mass, it retains a roughly constant offset against gut capacity. Analytical approximation and simulation results are denoted by circles and squares, respectively. The black line denotes the 1:1 line.

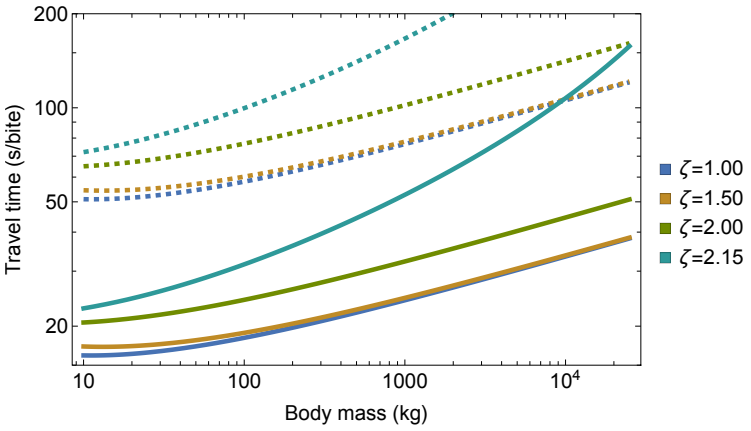


Figure S4: Travel time between bites during the forager's bout for different values of the patchiness exponent ζ (colors) in *i*) an environment with relatively more resources (solid lines; $\mu = 10^{-3.5}$) and *ii*) an environment with relatively fewer resources (stippled lines; $\mu = 10^{-4.0}$).

Supplemental Material (not copyedited or formatted) for: Justin D. Yeakel, Mason Fan, Emily Jane McTavish, Anna Carolina de Almeida, Christopher P. Kempes, Luís M. A. Bettencourt, Sora Kim, Greg Breed. 2026. "An Origin for the Allometric Scaling of Mammalian Fat Reflects Populations Living on the Edge." The American Naturalist 208(5). DOI: https://doi.org/10.1086/742753.

1997) are unavailable to us. So while we use approximations based on $\mathbb{E}\{N_e\}$ to showcase certain behaviors of our model (see main text figs. 3, 4), our interpretations of model results are primarily based on direct simulation output rather than analytical approximations.

Most of the scaling relationships incorporated into our foraging model are either well known (such as the scaling of metabolic rate), or based on clear biophysical dimensional constraints (the scaling of reaction width and height, forager velocity, and volumetric measures such as bite size and gut capacity). Some allometric relationships, however, are less well known or clearly understood, such as the scaling of foraging bout time with forager body mass (Owen-Smith, 1988). To ensure that our results are not strongly contingent on this scaling relationship, we present a sensitivity analysis, where $t_\mathrm{b} \propto M^{tb_1(1+\chi)}$ where $\chi \in (-0.5, 0.5)$ (Fig. S5). This shows that the gain surplus exponent is robust even in the face of large differences in the scaling of the foraging bout time with body mass.

Parameter	Meaning	Units	Value(s)
g	Daily energetic gains	$\mathrm{kJ \cdot day^{-1}}$	$g_0 M^{g_1}$
c	Daily energetic costs	$\mathrm{kJ \cdot day^{-1}}$	$c_0 M^{c_1}$
t_bout	Foraging bout time	s	$tb_0 M^{tb_1}$
tb_0	Foraging bout const.	$\mathrm{s \cdot kg^{-tb_1}}$	18220
tb_1	Foraging bout exp.	–	0.124
t_chew	Chewing time	s	$tc_0 M^{tc_1}$
tc_0	Chewing time const.	$\mathrm{s \cdot kg^{-tc_1}}$	0.267
tc_1	Chewing time exp.	–	0.196
u	Gut capacity	kJ	$\delta u_0 M^{u_1}$
u_0^ca	Caecum gut const.	$\mathrm{g \cdot kg^{-u_1}}$	0.025
u_0^co	Colon gut const.	$\mathrm{g \cdot kg^{-u_1}}$	0.029
u_0^nrf	Non-rumen foregut const.	$\mathrm{g \cdot kg^{-u_1}}$	0.030
u_0^rf	Rumen foregut const.	$\mathrm{g \cdot kg^{-u_1}}$	0.041
u_1^ca	Caecum gut exp.	–	0.860
u_1^co	Colon gut exp.	–	0.919
u_1^nrf	Non-rumen foregut exp.	–	0.881
u_1^rf	Rumen foregut exp.	–	0.897
B	Basal metabolic rate	$\mathrm{kJ \cdot s^{-1}}$	$B_0 M^{B_1}$
B_0	Basal metabolic rate const.	$(\mathrm{kJ \cdot s^{-1}}) \cdot \mathrm{kg^{-B_1}}$	0.0032
B_1	Basal metabolic rate exp.	–	0.75
F	Field metabolic rate	$\mathrm{kJ \cdot s^{-1}}$	$F_0 M^{F_1}$
F_0	Field metabolic rate const.	$(\mathrm{kJ \cdot s^{-1}}) \cdot \mathrm{kg^{-F_1}}$	0.0084
F_1	Field metabolic rate exp.	–	0.75

Table S3: Foraging parameters, definitions, units, and values. ca = caecum; co = colon; nrf = non-rumen foregut; rf = rumen foregut.

Supplemental Material (not copyedited or formatted) for: Justin D. Yeakel, Mason Fan, Emily Jane McTavish, Anna Carolina de Almeida, Christopher P. Kempes, Luís M. A. Bettencourt, Sora Kim, Greg Breed. 2026. "An Origin for the Allometric Scaling of Mammalian Fat Reflects Populations Living on the Edge." The American Naturalist 208(5). DOI: https://doi.org/10.1086/742753.

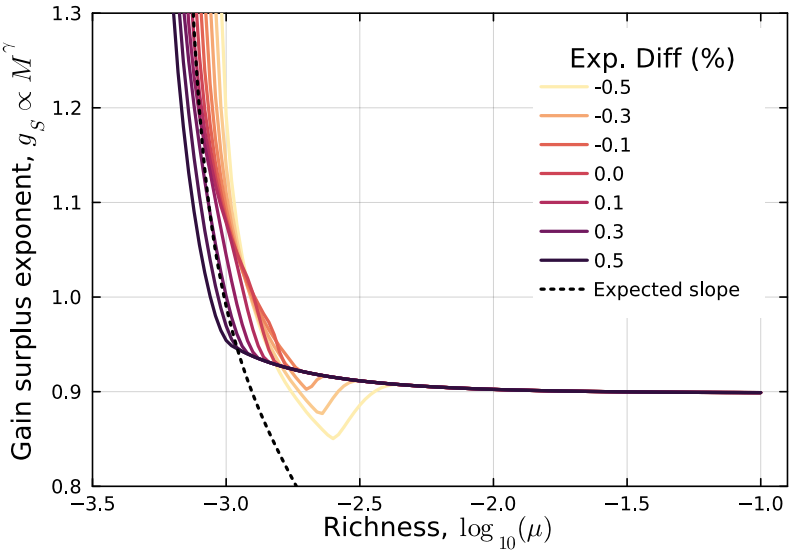


Figure S5: The gain surplus exponent γ as a function of resource density (μ) for caecum fermenters, where a degree of error has been applied to the allometric scaling of bout time (tb_1), such that $t_b \propto M^{tb_1(1+\chi)}$ where $\chi \in (-0.5, 0.5)$. Analytical approximation of γ (dotted line) is shown for resource-limited conditions for $\chi = 0$ (i.e., as calculated in the main text). The changes to the $\gamma \sim \mu$ curve are quantitative in nature, such that the notion that γ becomes superlinear in resource-limited environments is not altered by changing the scaling of the bout time with body mass. What this does impact is exactly where along μ this superlinearity is achieved, though the shift in values is not particularly striking.

D Food quality and biomass density

We do not include the relationship between resource quality and biomass density in our focal analysis presented in the main text, and will show here *i*) why this relationship is not expected to alter the nature of our results, and *ii*) verify this expectation with additional simulations. Forage quality is well-known to decline as forage biomass density increases (Fryxell, 1991), and this is expected to impact the total energetic intake by herbivorous mammals. For example, Bergman et al. (2001) explored this relationship with regard to bison foraging, where they found that proportional digestibility of plant resources, θ, declined roughly monotonically with plant

Supplemental Material (not copyedited or formatted) for: Justin D. Yeakel, Mason Fan, Emily Jane McTavish, Anna Carolina de Almeida, Christopher P. Kempes, Luís M. A. Bettencourt, Sora Kim, Greg Breed. 2026. "An Origin for the Allometric Scaling of Mammalian Fat Reflects Populations Living on the Edge." The American Naturalist 208(5). DOI: https://doi.org/10.1086/742753.

biomass density, μ ($\mathrm{g} \cdot \mathrm{m}^{-2}$), where in this case $\theta(\mu) = \theta_0 - \theta_1\mu$, with $\theta_0 = 0.68$ and $\theta_1 = 2.46 \times 10^{-3}$.

We show with eq. S6 that the number of encounters is inversely proportional to expected travel time. If we assume that chewing time is negligible when compared against travel time (as is expected, particularly in resource scarce environments where travel between bites is longer), we can state that $\mathbb{E}\{N_e\} \approx t_{\text{bout}}/\mathbb{E}\{T_{\text{travel}}\}$. From eq. S4, this means that $\mathbb{E}\{N_e\} \propto\!\!\!\sim \mu$ (because $q = \mu/\beta$). When herbivore gains are limited by the number of encounters that they have within a foraging bout, forage gains are calculated as $\mathbb{E}\{G\} = \delta\beta\mathbb{E}\{N_e\}$. If we include the effects of digestibility, this becomes $\mathbb{E}\{G\} = \theta(\mu)\delta\beta\mathbb{E}\{N_e\}$, such that $\mathbb{E}\{G\} \propto\!\!\!\sim \theta(\mu)\mu$.

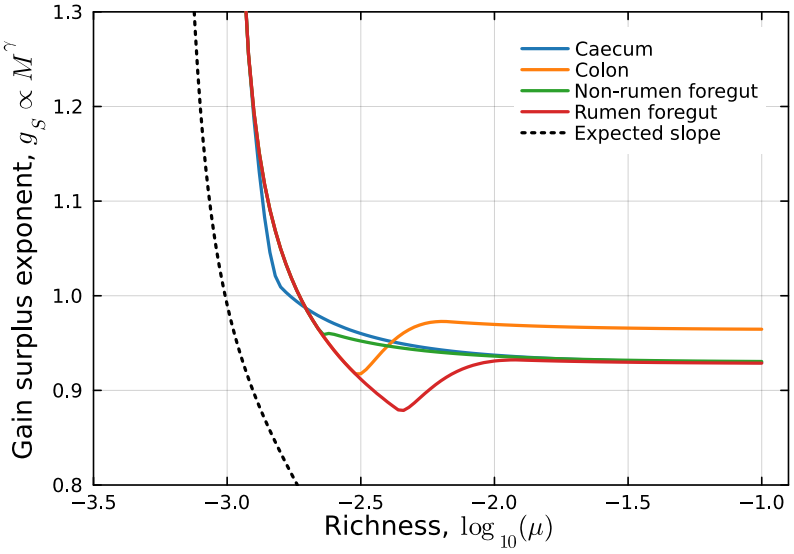


Figure S6: Daily gain surplus exponent γ as a function of environmental richness μ for caecum, colon, non-rumen foregut, and rumen foregut foragers, derived from simulations (500 replicates), with the negative relationship between digestibility and resource biomass density $\theta(\mu) = \theta_0 - \theta_1\mu$ included (following Bergman et al., 2001). Analytical approximation of γ is shown for resource-limited conditions without $\theta(\mu)$ (i.e., as calculated in the main text) to show how including $\theta(\mu)$ warps the gain surplus relationship along the μ axis, but does not alter the nature of the results.

In the main text, we assume that $\theta(\mu)$ does not vary with μ, such that gains increase linearly

Supplemental Material (not copyedited or formatted) for: Justin D. Yeakel, Mason Fan, Emily Jane McTavish, Anna Carolina de Almeida, Christopher P. Kempes, Luís M. A. Bettencourt, Sora Kim, Greg Breed. 2026. "An Origin for the Allometric Scaling of Mammalian Fat Reflects Populations Living on the Edge." The American Naturalist 208(5). DOI: https://doi.org/10.1086/742753.

with resource biomass density, or $\mathbb{E}\{G\} \propto \mu$. If instead $\theta(\mu)$ is assumed to decrease linearly with μ, we obtain $\mathbb{E}\{G\} \propto (\theta_0 - \theta_1\mu)\mu$, which is concave-down parabolic across μ. The relationship is thus roughly linear in the low-μ regime, reaches a maximum at $\mu^* = \frac{\theta_0}{2\theta_1}$, and then declines. Using the specific parameterization for the digestibility of sedges (*Carex* spp.) as a function of biomass density with respect to bison foragers, this maximum occurs at $\mu^* = 1.38 \times 10^3$ g $\cdot$ m^{-2}, which is far above the resource densities examined here, and firmly in the gut-limited rather than time-limited foraging regime. This is important because our primary mass-fat scaling results occur in resource scarce environments where foraging returns are limited by the number of bite encounters a forager has within a foraging bout, rather than the size of its gut. Furthermore, this means that gains are expected to remain roughly linearly increasing with μ, which aligns with the assumption of a constant digestibility across biomass density. We confirmed this expectation with an examination of model results with the $\theta(\mu)$ relationship from Bergman et al. (2001) included (fig. S6). This analysis shows that while including $\theta(\mu)$ adjusts where gain surplus g_S achieves superlinearity across μ (because gains are multiplied by the constant θ_0 in the low μ regime), it does not alter the overall relationship. This remains effectively unchanged even when the slope θ_1 is magnified (such that digestibility decreases more strongly with resource biomass density), and this again is due to the fact that in the low μ regime, expected gains are effectively linearly increasing with μ.

S3 From daily gain surplus to time-integrated fat storage

We currently calculate the daily gain surplus [kJ day^{-1}] as $g_S = g - c$, where in resource-limited environments $g \equiv g^{\text{bout}}$ represents acquired daily gains within a foraging bout, and c represents daily metabolic costs. Our simulation results reveal that g and c follow single power-law scaling relationships as a function of body mass M, where $g^{\text{bout}} = g_0 M^{g_1}$ and $c = c_0 M^{c_1}$. The effective slope of the gain surplus, where $g_S \propto M^{\gamma}$, is then calculated as

$$\gamma = g_1 + \frac{(c_1 - g_1)c_0 M^{c_1}}{c_0 M^{c_1} - g_0 M^{g_1}}. \tag{S7}$$

Supplemental Material (not copyedited or formatted) for: Justin D. Yeakel, Mason Fan, Emily Jane McTavish, Anna Carolina de Almeida, Christopher P. Kempes, Luís M. A. Bettencourt, Sora Kim, Greg Breed. 2026. "An Origin for the Allometric Scaling of Mammalian Fat Reflects Populations Living on the Edge." The American Naturalist 208(5). DOI: https://doi.org/10.1086/742753.

See the description around eq. 3 in the main text for additional details. This daily gain is interpreted as a reflection of fat, and it is stated that the allometric exponent of daily gain is expected to be equivalent to the allometric exponent of fat storage. We next derive the conditions for this assertion, and specify under what cases this assertion is expected to be robust, and under what cases it is expected to be altered.

Fat storage, S, is different from the energetic surplus of daily gains, g_S. A proportion of the daily gain surplus (which we assume is size-independent, based on the size-independence of herbivore digestive efficiency (Clauss and Hummel, 2005)) is routed to fat storage, but storage itself is integrated over a period of time. As such, we can state that $S(M) = g_S(M)\tau(M)$, where τ is the time over which fat stores are accumulated, which may or may not be dependent on body mass. Because we are here focused on investigating the scaling exponent of fat storage, for simplicity we will assume that the full g_S is routed to fat storage, though in practice this would be instead a proportion of g_S, and would not alter the following derivation.

If the timescale of fat accumulation is deterministic and independent of mass, we would expect the allometric exponent of gain surplus, γ, to be equivalent to the allometric exponent of storage. If, however, the timescale of fat accumulation is deterministic and mass-dependent, where a natural choice would be $\tau \propto M^{0.25}$ (Calder III, 1996), fat storage would instead scale as $S \propto M^{\gamma+0.25}$. Because expectations for γ are dependent on environmental richness, this change to the exponent would then shift the function shown in fig. 4 (main text) upwards by 0.25 units. As we have described for other scaling changes that alter at what value of μ superlinearity is achieved without altering the achievement of superlinearity, our qualitative findings would remain unchanged.

However, the dynamics of storage is not a deterministic process, but is instead both stochastic and seasonal. We will address temporal sequences of surplus and deficit more below, but for now will focus on seasons of surplus, where accumulation is possible. We will explore two possible modes of fat accumulation: 1) where gain surplus is stochastically added to surplus, but where the mean storage amount is zero (diffusion-dominated storage), which we deem less relevant;

Supplemental Material (not copyedited or formatted) for: Justin D. Yeakel, Mason Fan, Emily Jane McTavish, Anna Carolina de Almeida, Christopher P. Kempes, Luís M. A. Bettencourt, Sora Kim, Greg Breed. 2026. "An Origin for the Allometric Scaling of Mammalian Fat Reflects Populations Living on the Edge." The American Naturalist 208(5). DOI: https://doi.org/10.1086/742753.

2) where gain surplus is stochastically added to surplus, and where the mean storage increases over time (drift-dominated storage), which is more relevant to our assumptions herein.

Diffusion-dominated storage. Here we assume that daily energetic balances fluctuate with mean zero and standard deviation $\sigma_g(M)$. We will assume a ruin probability $\leq \epsilon$ over the time horizon τ, where 'ruin probability' means the chance that reserves are exhausted at any time within $[0, \tau]$. Storage then is assumed to change as

$$X(t) = S_0 + \sigma_g W(t), \tag{S8}$$

where S_0 is the starting stock (our fat reserves), and $W(t)$ is Brownian motion. We want to find the probability of ruin in $[0, \tau]$. Using first-passage results, the minimum starting stock required to keep ruin probability below ϵ is approximately

$$S_0(M) \approx \psi \sigma_g(M) \sqrt{\tau(M)}, \tag{S9}$$

where the safety factor $\psi = \Psi^{-1}(1 - \epsilon/2)$, assuming $\Psi(\cdot)$ is the normal CDF. The safety factor describes how many day-to-day standard deviations of buffer a forager must carry to keep the chance of depleting reserves below ϵ. A smaller ϵ therefore implies a rarer failure event, which translates into a larger ψ (a larger cushion). Assuming the standard deviation of daily gain is of the same order as the mean daily gain, such that $\sigma_g(M) \propto M^{\gamma}$, this will mean that $S_0(M) \propto M^{\gamma + 0.125}$. So when the energetic gains routed to fat are dominated by diffusion dynamics without drift, the allometric exponent of the required fat buffer is expected to be greater than that of daily gain surplus, or $\gamma + 0.125$.

Stochastic accumulation with drift. Our foraging model and assumptions throughout occupy a space where there is consistant gain surplus. In this regime, stochastic accumulation would not be expected to be diffusion-dominated, but drifting upwards. Of course, this can't go on forever (dietary habits in the U.S. notwithstanding), which we will address in more detail below. Here

Supplemental Material (not copyedited or formatted) for: Justin D. Yeakel, Mason Fan, Emily Jane McTavish, Anna Carolina de Almeida, Christopher P. Kempes, Luís M. A. Bettencourt, Sora Kim, Greg Breed. 2026. "An Origin for the Allometric Scaling of Mammalian Fat Reflects Populations Living on the Edge." The American Naturalist 208(5). DOI: https://doi.org/10.1086/742753.

Parameter	Meaning	Units	Value(s)
$X(t)$	Fat stores trajectory	kJ	–
S_0	Starting reserves	kJ	–
$\widehat{g_S}(M)$	Mean gain surplus	$\text{kJ} \cdot \text{day}^{-1}$	
$\sigma(M)$	Std. dev. gain surplus	$\text{kJ} \cdot \text{day}^{-1/2}$	$\sigma_0 M^{\gamma_\sigma}$
$\tau(M)$	Accumulation window	day	$\tau_0 M^{\tau_1}$
τ_0	Time const.	$\text{day} \cdot \text{kg}^{-\tau_1}$	–
τ_1	Time exp.	–	≤ 0.25
$W(t)$	Standard Wiener process	$\text{day}^{1/2}$	–
ϵ	Ruin probability tolerance	–	0.05
Ψ	Standard normal CDF	–	–
ψ	Safety factor $\Psi^{-1}(1-\epsilon/2)$	–	1.96
x	Reserves in volatility units	–	$S_0/(\sigma\sqrt{\tau})$
a	Surplus signal-noise ratio	–	$\widehat{g_S}\sqrt{\tau}/\sigma$
$S_{\text{burn}}(M)$	Minimal reserve for burn	kJ	–
$S_{\text{risk}}(M)$	Minimal reserve for risk ϵ	kJ	–
M^*	Crossover mass	kg	–

Table S4: Stochastic fat accumulation parameters, definitions, units, and values.

we will again assume a ruin probability $\leq \epsilon$ over the time horizon τ, where

$$X(t) = S_0 + \widehat{g_S} t + \sigma W(t), \tag{S10}$$

where S_0 is the starting stock (our fat reserves), and $W(t)$ is Brownian motion, and $\widehat{g_S}$ is our mean daily surplus. The finite-horizon ruin probability, from the first passage result based on Brownian motion with drift (Darling and Siegert, 1953), is then written

$$\begin{aligned} \text{Pr}_{\text{ruin}}(S_0) = &\exp\left(-\frac{2\widehat{g_S}S_0}{\sigma^2}\right)\Psi\left(-\frac{S_0 - \widehat{g_S}\tau}{\sigma\sqrt{\tau}}\right) \\ &+ \Psi\left(-\frac{S_0 + \widehat{g_S}\tau}{\sigma\sqrt{\tau}}\right), \end{aligned} \tag{S11}$$

where setting this equal to ϵ, and using $x = \frac{S_0}{\sigma\sqrt{\tau}}$ and $a = \frac{\widehat{g_S}\sqrt{\tau}}{\sigma}$, we get the dimensionless

$$\begin{aligned} f(x|a) &= \exp(-2ax)\Psi(-(x-a)) \\ &\quad + \Psi(-(x+a)) - \epsilon \\ &= 0. \end{aligned} \tag{S12}$$

We note that both x and a have specific biological interpretations. The composite variable x is effectively the starting reserves in units of seasonal volatility, or in other words how many standard deviations of cumulative day-to-day uncertainty the initial fat reserves S_0 can absorb

Supplemental Material (not copyedited or formatted) for: Justin D. Yeakel, Mason Fan, Emily Jane McTavish, Anna Carolina de Almeida, Christopher P. Kempes, Luís M. A. Bettencourt, Sora Kim, Greg Breed. 2026. "An Origin for the Allometric Scaling of Mammalian Fat Reflects Populations Living on the Edge." The American Naturalist 208(5). DOI: https://doi.org/10.1086/742753.

over the upcoming temporal interval τ. Along similar lines, the composite variable a represents a dimensionless seasonal surplus signal-to-noise ratio, where the expected surplus accumulated over the window is $\widehat{g_S}\tau$, while its random fluctuation is $\sigma\sqrt{\tau}$. As $a = (\widehat{g_S}\tau)/(\sigma\sqrt{\tau}) = \frac{\widehat{g_S}\sqrt{\tau}}{\sigma}$, this value describes how many standard-deviation units of reserve can be stored over the temporal interval associated with storage. Because larger mammals can store greater amounts of fat, a is expected to increase with body mass.

There are two asymptotic regimes to the above formulation: a small-a regime (typically smaller body masses), which is diffusion-dominated, and a large-a regime (typically larger body masses), which is drift-dominated. The cross-over to this regime occurs at $a(M^*) = \frac{\log(1/\epsilon)}{2\psi}$, where ψ again is the safety factor $\psi = \Psi^{-1}(1-\epsilon/2)$. Solving for the cross-over mass where diffusion-dominance switches to drift-dominance, we get

$$M^* = \left(\frac{\log(1/\epsilon)}{2\psi}\frac{\sigma_0}{g_0\sqrt{\tau_0}}\right)^{1/(\gamma_{\widehat{g_S}}-\gamma_\sigma+\tau_1/2)}, \tag{S13}$$

where g_0, σ_0, τ_0 are prefactors for the gain surplus, standard deviation of surplus, and time horizon scaling relationships, respectively, and $\gamma_{\widehat{g_S}}$, γ_σ, and τ_1 are the respective allometric exponents. The prefactor for M^* will be $\ll 1$ generally speaking, given that μ_0 and σ_0 are of the same order, the default $\frac{\log(1/\epsilon)}{2\psi} = 0.76$ where $\epsilon = 0.05$ meaning $\psi = 1.96$, while $\sqrt{\tau_0}$ will be large. The exponent for M^* is large, roughly $1/0.125 = 8$. This means the cross-over mass M^* will be considerably smaller than the smallest mammal, such that mammalian stores will generally follow drift-dominated storage dynamics rather than diffusion-dominated storage dynamics. See fig. S7 for the approximations of the two asymptotic regimes.

In a drift-dominated system, where a is very large, we approximate

$$f(x|a \gg \psi) \approx \exp(-2ax), \tag{S14}$$

such that

$$S_0(M) \approx \frac{\sigma^2}{2\widehat{g_S}}\log\left(\frac{1}{\epsilon}\right). \tag{S15}$$

Assuming the mean daily surplus and standard deviation of the daily surplus are of the same order (i.e. that $\gamma \equiv \gamma_\sigma = \gamma_{\widehat{g_S}}$), we obtain the scaling $S_0(M) \propto M^\gamma$. So when storage accumulates

Supplemental Material (not copyedited or formatted) for: Justin D. Yeakel, Mason Fan, Emily Jane McTavish, Anna Carolina de Almeida, Christopher P. Kempes, Luís M. A. Bettencourt, Sora Kim, Greg Breed. 2026. "An Origin for the Allometric Scaling of Mammalian Fat Reflects Populations Living on the Edge." The American Naturalist 208(5). DOI: https://doi.org/10.1086/742753.

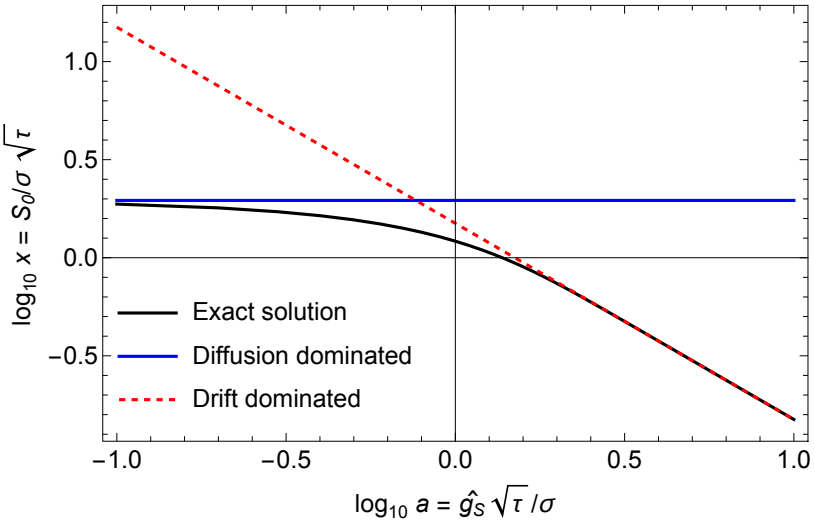


Figure S7: Required starting fat versus surplus-variability ratio for a fixed ruin tolerance $\epsilon = 0.05$, where the starting reserves in units of seasonal volatility, x, varies as a function of the seasonal surplus signal-to-noise ratio, a. The black curve represents the exact solution x of eq. S12. The blue line is the diffusion asymptote approximation, while the red line is the drift asymptote approximation. As a increases, x declines, as the mean surplus dominates the noise, such that less buffer is required to ensure the same risk of failure.

stochastically, and is dominated by drift, the allometric exponent of fat storage is expected to be equivalent to that of daily gain surplus, or γ.

Iterative periods of accumulation and deficit. We have so far shown that during periods of storage accumulation (where there is energetic surplus), fat storage is expected to scale equivalent to daily energetic gain, or $\propto M^{\gamma}$. However, individuals cannot always accumulate, such that periods are accumulation typically precede periods of deficit, where stored reserves are utilized. We show below that iterative periods of accumulation and deficit are also expected to scale $\propto M^{\gamma}$ in the general case. We suspect that a more holistic and rigorous investigation of how cycles of accumulation and utilization occur in uncertain environments may uncover a more general suite of relationships governing biological storage processes, which we leave for a future investigation.

Supplemental Material (not copyedited or formatted) for: Justin D. Yeakel, Mason Fan, Emily Jane McTavish, Anna Carolina de Almeida, Christopher P. Kempes, Luís M. A. Bettencourt, Sora Kim, Greg Breed. 2026. "An Origin for the Allometric Scaling of Mammalian Fat Reflects Populations Living on the Edge." The American Naturalist 208(5). DOI: https://doi.org/10.1086/742753.

Consider two phases within a typical annual cycle: (i) a surplus interval during which reserves are accumulated, and (ii) a deficit interval during which reserves are expended.

Deficit interval with deterministic burn. Here we assume negligible intake during the deficit period, so that reserves decline deterministically with the daily metabolic rate

$$c(M) = c_0 M^{c_1}, \tag{S16}$$

where $c_1 \approx 0.75$, over a deficit duration

$$\tau(M) = \tau_0 M^{\tau_1}, \tag{S17}$$

where $\tau_1 \leq 0.25$. The stores required to cover this deterministic burn are then calculated as

$$S_{\text{burn}}(M) = c(M)\tau(M) = c_0 \tau_0 M^{c_1+\tau_1}, \tag{S18}$$

so the corresponding allometric exponent is $c_1 + \tau_1 \leq 1$.

Surplus interval with stochastic drift-dominated storage. With $\widehat{g_S}(M)$ and $\sigma(M)$ again denoting the mean and standard deviation of the daily surplus, in the drift-dominated first-passage regime (see previous section), the minimal pre-deficit reserve that limits ruin to probability ϵ is

$$S_{\text{risk}}(M) = \frac{\sigma^2}{2\widehat{g_S}} \log\left(\frac{1}{\epsilon}\right). \tag{S19}$$

If $\widehat{g_S}$ and σ share the same allometric exponent (size-invariant daily CV),

$$\widehat{g_S}(M) \propto M^{\gamma_{\widehat{g_S}}}, \text{ and } \sigma(M) \propto M^{\gamma_\sigma}, \tag{S20}$$

and $\gamma_\sigma \simeq \gamma_{\widehat{g_S}} \equiv \gamma$, as we have already assumed. This allows us to write

$$S_{\text{risk}}(M) \propto M^{2\gamma_\sigma - \gamma_{\widehat{g_S}}} \approx M^{\gamma}. \tag{S21}$$

And, as before, γ is the exponent of the gain surplus, where, in the resource-limited case we have $\gamma > 1$.

Supplemental Material (not copyedited or formatted) for: Justin D. Yeakel, Mason Fan, Emily Jane McTavish, Anna Carolina de Almeida, Christopher P. Kempes, Luís M. A. Bettencourt, Sora Kim, Greg Breed. 2026. "An Origin for the Allometric Scaling of Mammalian Fat Reflects Populations Living on the Edge." The American Naturalist 208(5). DOI: https://doi.org/10.1086/742753.

The necessary reserve target at the onset of the deficit period is the binding minimum required to satisfy both constraints,

$$S^*(M) \approx \max\left\{S_{\text{burn}}(M), S_{\text{risk}}(M)\right\}. \tag{S22}$$

Consequently, the asymptotic fat mass exponent is

$$\Gamma = \max\left\{\gamma, c_1 + \tau_1\right\}. \tag{S23}$$

In the regimes we emphasize ($\gamma > 1$ and $c_1 + \tau_1 \leq 1$), the resulting exponent is $\Gamma = \gamma$.

If the deficit interval itself is stochastic, two limits obtain for the reserve needed to survive the deficit phase: (i) for short, random deficits (high recovery rate), erosion is diffusion-like, $S_{\text{deficit}}(M) \propto \sigma(M)\sqrt{\tau(M)}$ with exponent $\gamma_\sigma + \tau_1/2$ (typically $\approx c_1 + \tau_1/2 < 1$); (ii) for long deficits (low recovery rate), erosion is effectively deterministic, $S_{\text{deficit}}(M) \propto c(M)\tau(M)$ with exponent $c_1 + \tau_1 \leq 1$. In either case the deficit-side exponents are linear or sub-linear and thus remain $< \gamma$ when $\gamma > 1$, so $S^*(M)$ inherits the surplus exponent.

S4 The reserve ratio accounting for demographic costs

We evaluate the reserve ratio $\phi = g/c$ in resource-limited environments, where both $g = g_0 M^{g_1}$ and $c = c_0 M^{c_1}$ are bout-limited, which we denote as g^{bout} and c^{bout}, respectively. As described in the main text, we view the gain surplus $g_S = g - c$ as a proxy for the energy foragers have available to them to direct to fat reserves, such that the scaling the g_S, denoted by γ, may be expected to scale simiarly as fat mass M_f as a function of body mass. In otherwords, we assume that $g_S \propto M^\gamma$ and $M_f \propto M^\gamma$. Assuming the observed value of $\gamma^* \equiv \gamma = 1.17$, we calculate the constrained reserve ratio

$$\phi|_{\gamma=\gamma^*} = \left.\frac{g^{\text{bout}}}{c^{\text{bout}}}\right|_{\gamma=\gamma^*} = 1 - \frac{c_1 - g_1}{\gamma^* - g_1}. \tag{S24}$$

The reserve ratio thus describes the relative gain equated with the observed mass-fat scaling relationship, and is independent of forager mass, depending only on the scaling exponents associated with gains and costs.

Supplemental Material (not copyedited or formatted) for: Justin D. Yeakel, Mason Fan, Emily Jane McTavish, Anna Carolina de Almeida, Christopher P. Kempes, Luís M. A. Bettencourt, Sora Kim, Greg Breed. 2026. "An Origin for the Allometric Scaling of Mammalian Fat Reflects Populations Living on the Edge." The American Naturalist 208(5). DOI: https://doi.org/10.1086/742753.

Parameter	Meaning	Units	Value(s)
ϕ	Reserve ratio	–	g/c
κ	Per-diem demographic costs	kJ day^{-1}	$\kappa_0 M^{\kappa_1}$
κ_{growth}	Per-diem growth costs	kJ day^{-1}	var.
κ_{rep}	Per-diem reproductive costs	kJ day^{-1}	var.
κ_0	Per-diem demo. costs const.	(kJ day^{-1})$^{1-\kappa_1}$	86.66
κ_1	Per-diem demo. costs exp.	–	0.748
t_ℓ	Generational time	days	var.
b_1	Birth mass exp.	–	0.92
m_0	Birth mass	kg	$b_0 M^{b_1}$
b_0	Birth mass const.	kg$^{1-b_1}$	55.81
b_1	Birth mass exp.	–	0.92
E_m	Energetic cost of synthesis	kJ kg^{-1}	5774

Table S5: Demographic parameters, definitions, units, and values.

As discussed in the main text, the daily costs associated with foraging are not the only costs demanded of organisms operating within a stable population. Additional costs include *i*) the energetic cost of growing to adult size M, and *ii*) the energetic cost of replacement, which is at minimum two offspring for sexually-reproducing females. We account for these demographic costs by calculating a daily demographic expenditure, which is effectively the total cost of growth and reproduction divided by the expected number of days within a generational timescale. The daily demographic costs are thus

$$\begin{aligned} \kappa &= \kappa_{\text{growth}} + \kappa_{\text{rep}}, \\ &= \frac{c_{\text{growth}}}{t_\ell} + \frac{c_{\text{rep}}}{t_\ell}. \end{aligned} \tag{S25}$$

Both the generational time and the ontogenetic costs of growth are calculated from the metabolic balance equation (West et al., 2001)

$$B_0 m^{3/4} = E_m \dot{m} + B_m m, \tag{S26}$$

where m is the size of the forager as it grows to its adult body mass M, $\dot{m}$ is the time derivative of m, E_m is the energetic cost of tissue synthesis [kJ/kg], and B_m is the energetic cost of tissue maintenance. The generation time t_ℓ follows the time solution to eq. S26, such that

$$t_\ell = \ln \left[\frac{1 - (m_0/M)^{1/4}}{1 - \frac{M_r}{M}^{1/4}} \right] \frac{M^{1/4}}{a/4}, \tag{S27}$$

Supplemental Material (not copyedited or formatted) for: Justin D. Yeakel, Mason Fan, Emily Jane McTavish, Anna Carolina de Almeida, Christopher P. Kempes, Luís M. A. Bettencourt, Sora Kim, Greg Breed. 2026. "An Origin for the Allometric Scaling of Mammalian Fat Reflects Populations Living on the Edge." The American Naturalist 208(5). DOI: https://doi.org/10.1086/742753.

where M_r is the reproductive mass (here assumed to be $0.99M$), $a = B_0/E_m$, and m_0 is birth mass, where $m_0 = b_0 M^{b_1}$, and scales approximately as $t_\ell \propto M^{0.25}$ (Yeakel et al., 2018). The energetic cost of growth from birth mass m_0 to adult mass $\epsilon_A M$ (where M is the asymptotic mass, and $\epsilon_A = 0.99$) is then calculated as

$$c_{\text{growth}} = \int_{m_0}^{\text{ffl}_\text{A}\text{M}} E_m \dot{m} \text{dt} = E_m(\epsilon_A M - m_0). \tag{S28}$$

The energetic cost of giving birth to two individuals and fueling their growth to size $\epsilon_J M$ (where $\epsilon_J = 0.75$ represents the end of the juvenile period) is then calculated in a very similar way, where

$$c_{\text{rep}} = 2\int_{0}^{\text{ffl}_\text{J}\text{M}} E_m \dot{m} \text{dt} = 2E_m \epsilon_J M. \tag{S29}$$

Combined, we have

$$\kappa = \frac{E_m(\epsilon_A M - m_0 + 2\epsilon_J M)}{t_\ell} \tag{S30}$$

Importantly, we observe that $\kappa = \kappa_0 M^{\kappa_1}$ (fig. S8). Modifying eq. S24 to include daily demographic costs, we obtain

$$\begin{aligned} \phi|_{\gamma=\gamma^*} = \left.\frac{g^{\text{bout}} - \kappa}{c^{\text{bout}}}\right|_{\gamma=\gamma^*} &= 1 - \frac{c_1 - g_1}{\gamma^* - g_1} - \frac{\kappa}{c^{\text{bout}}}. \\ &= 1 - \frac{c_1 - g_1}{\gamma^* - g_1} - \frac{\kappa_0 M^{\kappa_1}}{c_0 M^{c_1}}. \end{aligned} \tag{S31}$$

Because $\kappa_1 \approx c_1$, this simplifies to

$$\phi|_{\gamma=\gamma^*} = \left.\frac{g^{\text{bout}} - \kappa}{c^{\text{bout}}}\right|_{\gamma=\gamma^*} = 1 - \frac{c_1 - g_1}{\gamma^* - g_1} - \frac{\kappa_0}{c_0}, \tag{S32}$$

where $\kappa_0/c_0 = 0.24$, meaning that 24% of daily energetic gains relative to costs represent sunk costs associated with growth and reproduction. While g_1 and c_1 can vary depending on the resource environment (though c_1 varies much less than g_1), in the regime where the observed mass-fat scaling occurs, we calculate $\phi^{\text{dem}} \approx 1.37$. This means that if herbivores – regardless of body size – reach a 37% forage surplus after accounting for demographic costs, they will have met the minimal conditions needed to maintain population stability and to have attained the observed mass-fat scaling relationship.

Supplemental Material (not copyedited or formatted) for: Justin D. Yeakel, Mason Fan, Emily Jane McTavish, Anna Carolina de Almeida, Christopher P. Kempes, Luís M. A. Bettencourt, Sora Kim, Greg Breed. 2026. "An Origin for the Allometric Scaling of Mammalian Fat Reflects Populations Living on the Edge." The American Naturalist 208(5). DOI: https://doi.org/10.1086/742753.

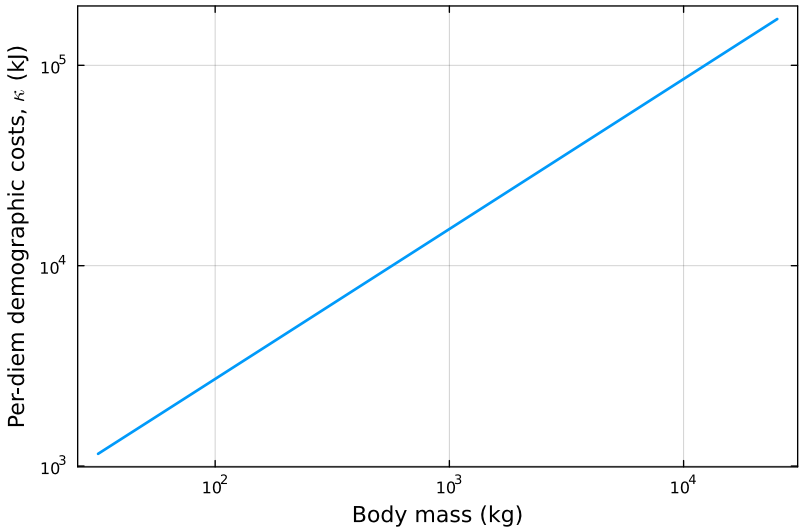


Figure S8: Per-diem demographic costs κ [kJ] as a function of body mass M. This relationship follows the allometric scaling $\kappa = 86.66M^{0.748}$, such that the relative demographic cost $\kappa/c \approx 0.24$ is a constant.

S5 The reserve ratio with herbivore-induced patchiness

When $\zeta > 2$, the patchiness of the underlying resource distribution increases with herbivore body mass. As described in the main text, this may be expected in highly engineered landscapes or when large species must travel between food islands. Furthermore, we demonstrate that the reserve ratio $\phi = g/c$ increases more shallowly with body size with $\zeta > 2$, reaching a maximum at intermediate size class (at ca. $M = 2000$ kg for $\zeta = 2.15$) before declining (teal line, main text fig. 3B).

We show here a more continuous perspective of the effect of increasing ζ with the condition that $\zeta > 2$ (fig. S9A). When $\zeta \approx 2$, we observe an increase in ϕ with increasing M similar to $\zeta < 2$ conditions (compare with main text fig. 3B). The slope of this relationship declines as ζ continues to increase, and becomes nonlinear when $\zeta \approx 2.11$, such that the ϕ is maximized at an intermediate body mass. The intermediate body mass at which ϕ is maximized declines as ζ continues to increase, and eventually $\phi < 1$ for all M, meaning that gains are not greater

Supplemental Material (not copyedited or formatted) for: Justin D. Yeakel, Mason Fan, Emily Jane McTavish, Anna Carolina de Almeida, Christopher P. Kempes, Luís M. A. Bettencourt, Sora Kim, Greg Breed. 2026. "An Origin for the Allometric Scaling of Mammalian Fat Reflects Populations Living on the Edge." The American Naturalist 208(5). DOI: https://doi.org/10.1086/742753.

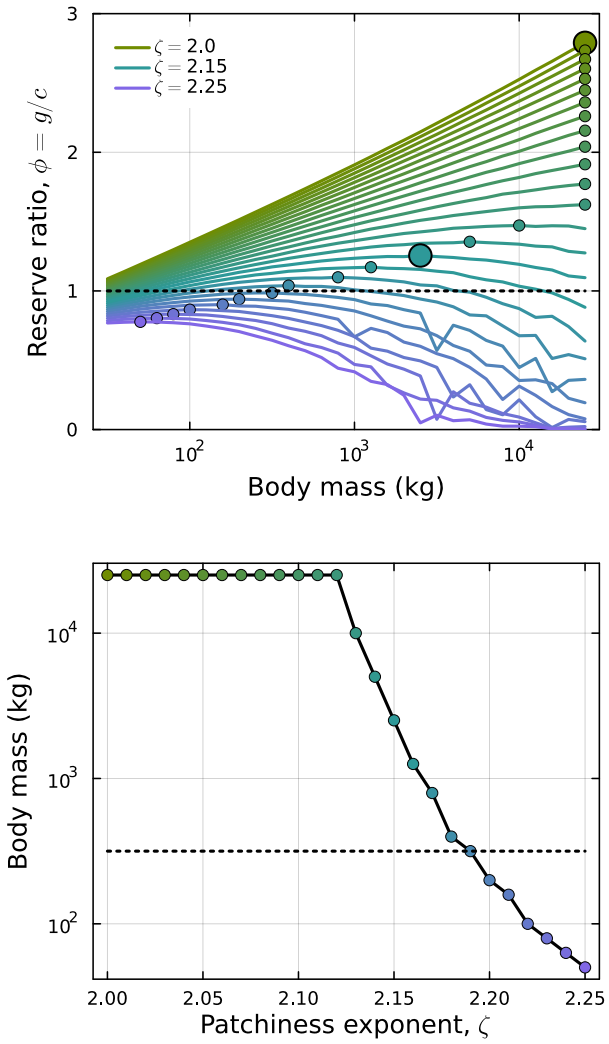


Figure S9: A. The reserve ratio $\phi = g/c$ for $\zeta > 2$, from simulation results. As ζ increases, the relationship become increasingly nonlinear as a function of body mass. This means that body masses that maximize the reserve ratio (points) decline to intermediate body size classes. The stippled line denotes where $\phi = 1$, below which daily energetic gains cannot account energetic costs. Herbivore foragers below this boundary for a given ζ are not considered feasible. The enlarged points show ϕ-maximizing body masses for ζ values used in the main text. B. Body masses that maximize ϕ as a function of ζ. The points are the same as those shown in panel A. The stippled line denotes the ϕ-maximizing body mass where $\phi = 1$; below this line, herbivores with these ϕ-maximizing body masses are not considered feasible.

Supplemental Material (not copyedited or formatted) for: Justin D. Yeakel, Mason Fan, Emily Jane McTavish, Anna Carolina de Almeida, Christopher P. Kempes, Luís M. A. Bettencourt, Sora Kim, Greg Breed. 2026. "An Origin for the Allometric Scaling of Mammalian Fat Reflects Populations Living on the Edge." The American Naturalist 208(5). DOI: https://doi.org/10.1086/742753.

than costs for any body mass. Under these conditions, we judge herbivory to be infeasible given that what is gained does not make up what is spent, and this is prior to accounting for sunk demographic costs (see app. S4). The declining relationship between the ϕ-maximizing body mass and patchiness exponent ζ is shown from a different perspective in fig. S9B.

Throughout we have observed that larger body sizes have a distinct energetic advantage with regard to traveling across a resource landscape to procure food. This emerges from a steeper gain relationship relative to costs, the consequence of being able to access more foods per unit time that emerges from a larger reaction cross-section and a higher per-bite encounter rate. However, when $\zeta > 2$, the coefficient of variation of the underlying resource distribution increases with body mass (fig. S2A), which may be due to the effect of those large herbivores on the spatial distributions of the resources themselves. Effectively, this means that there is more variability in the distances between bites for larger herbivores. For $\zeta > 2.10$, the gains relative to costs for the largest herbivores begin to decline, such that the ϕ-maximizing body mass is now at an intermediate size class.

In the current version of the foraging model, the resource distribution is set as an input driving the energetic consequences of herbivory. We suspect that if these dynamics were instead connected and allowed to feed back on one another, the high resource variability generated by such large body sizes could serve to generate selection for those herbivores able to maximize their gain relative to costs. If larger herbivores do indeed promote patchiness as is assumed with $\zeta > 2$, this would generate selection pressure against the largest herbivores, perhaps serving as a check on maximum body size. Such dynamics would have implications for our understanding of mammalian size-evolution throughout the Cenozoic, and in particular the impact of open habitats from closed forests roughly timing with the Eocene-Oligocene Transition (Strömberg, 2011), and accelerating at ca. 23 million years before present (Andermann et al., 2022). Minimal foraging frameworks, such as that presented here, may be useful for exploring the fitness consequences of such signficant global/climatological events on mammalian evolution (Rallings et al., 2024; Yeakel et al., 2024).

Supplemental Material (not copyedited or formatted) for: Justin D. Yeakel, Mason Fan, Emily Jane McTavish, Anna Carolina de Almeida, Christopher P. Kempes, Luís M. A. Bettencourt, Sora Kim, Greg Breed. 2026. "An Origin for the Allometric Scaling of Mammalian Fat Reflects Populations Living on the Edge." The American Naturalist 208(5). DOI: https://doi.org/10.1086/742753.

Literature Cited

Andermann, T., C. A. E. Strömberg, A. Antonelli, and D. Silvestro. 2022. The origin and evolution of open habitats in north america inferred by bayesian deep learning models. Nature Communications 13:4833.

Bergman, C. M., J. M. Fryxell, C. C. Gates, and D. Fortin. 2001. Ungulate foraging strategies: energy maximizing or time minimizing? Journal of Animal Ecology 70:289–300.

Bhat, U., C. P. Kempes, and J. D. Yeakel. 2020. Scaling the risk landscape drives optimal life-history strategies and the evolution of grazing. Proc. Natl. Acad. Sci. U.S.A. 117:1580–1586.

Calder III, W. A. 1996. Size, function, and life history. Courier Corporation.

Clauss, M., and J. Hummel. 2005. The digestive performance of mammalian herbivores: why big may not be that much better. Mammal Review 35:174–187.

Damuth, J. 1987. Interspecific allometry of population density in mammals and other animals: the independence of body mass and population energy-use. Biol. J. Linn. Soc. 31:193–246.

Darling, D. A., and A. J. Siegert. 1953. The first passage problem for a continuous markov process. The Annals of Mathematical Statistics pages 624–639.

Denny, M. 2017. The fallacy of the average: on the ubiquity, utility and continuing novelty of jensen's inequality. Journal of Experimental Biology 220:139–146.

Fryxell, J. M. 1991. Forage quality and aggregation by large herbivores. The American Naturalist 138:478–498.

George, J. C., J. R. Bockstoce, A. E. Punt, and D. B. Botkin. 2007. Preliminary estimates of bowhead whale body mass and length from yankee commercial oil yield records. Center for the Study of the Environment 98105:5020.

Supplemental Material (not copyedited or formatted) for: Justin D. Yeakel, Mason Fan, Emily Jane McTavish, Anna Carolina de Almeida, Christopher P. Kempes, Luís M. A. Bettencourt, Sora Kim, Greg Breed. 2026. "An Origin for the Allometric Scaling of Mammalian Fat Reflects Populations Living on the Edge." The American Naturalist 208(5). DOI: https://doi.org/10.1086/742753.

Hilborn, R., and M. Mangel. 1997. The Ecological Detective: Confronting Models with Data. Monographs in Population Biology. Princeton University Press.

Holland, E., J. Aegerter, and C. Dytham. 2009. Comparing resource representations and choosing scale in heterogeneous landscapes. Landscape ecology 24:213–227.

Kramer, K., and H. Prins. 2010. Allometric scaling of resource acquisition by ruminants in dynamic and heterogeneous environments. Ecological Modelling 221:2555–2564.

Larramendi, A. 2015. Shoulder height, body mass, and shape of proboscideans. Acta Palaeontologica Polonica 61:537–574.

Lund, J., T. Smith, D. Chatwin, W. Sanger, J. T. duPasquier, and A. Kirkpatrick. 2025. American offshore whaling database. `https://whalinghistory.org/av/`. Accessed: 2025-05-05.

Müller, D. W., D. Codron, C. Meloro, A. Munn, A. Schwarm, J. Hummel, and M. Clauss. 2013. Assessing the jarman–bell principle: scaling of intake, digestibility, retention time and gut fill with body mass in mammalian herbivores. Comparative Biochemistry and Physiology Part A: Molecular & Integrative Physiology 164:129–140.

Navarrete, A., C. P. Van Schaik, and K. Isler. 2011. Energetics and the evolution of human brain size. Nature 480:91–93.

Owen-Smith, R. N. 1988. Megaherbivores: the influence of very large body size on ecology. Cambridge university press.

Pawar, S., A. I. Dell, and V. M. Savage. 2012. Dimensionality of consumer search space drives trophic interaction strengths. Nature .

Pitts, G. C., and T. R. Bullard. 1968. Some interspecific aspects of body composition in mammals. Pages 45–70 *in* N. R. Council, ed. Body Composition in Animals and Man. National Academy of Sciences, Washington, D.C.

Supplemental Material (not copyedited or formatted) for: Justin D. Yeakel, Mason Fan, Emily Jane McTavish, Anna Carolina de Almeida, Christopher P. Kempes, Luís M. A. Bettencourt, Sora Kim, Greg Breed. 2026. "An Origin for the Allometric Scaling of Mammalian Fat Reflects Populations Living on the Edge." The American Naturalist 208(5). DOI: https://doi.org/10.1086/742753.

Pond, C. M. 1978. Morphological aspects and the ecological and mechanical consequences of fat deposition in wild vertebrates. Annual Review of Ecology and Systematics 9:519–570.

Pond, C. M., and C. A. Mattacks. 1985. Body mass and natural diet as determinants of the number and volume of adipocytes in eutherian mammals. Journal of morphology 185:183–193.

Rallings, T., C. P. Kempes, and J. D. Yeakel. 2024. On the dynamics of mortality and the ephemeral nature of mammalian megafauna. Am. Nat. 204:274–288.

Ryg, M., C. Lydersen, L. Knutsen, A. Bjørge, T. Smith, and N. Øritsland. 1993. Scaling of insulation in seals and whales. Journal of Zoology 230:193–206.

Shipley, L. A., J. E. Gross, D. E. Spalinger, N. T. Hobbs, and B. A. Wunder. 1994. The scaling of intake rate in mammalian herbivores. Am. Nat. 143:1055–1082.

Strömberg, C. A. E. 2011. Evolution of Grasses and Grassland Ecosystems. Annu. Rev. Earth. Pl. Sc. 39:517–544.

West, G. B., J. H. Brown, and B. J. Enquist. 2001. A general model for ontogenetic growth. Nature 413:628–631.

Yeakel, J. D., M. C. Hutchinson, C. P. Kempes, P. L. Koch, J. L. Gill, and M. M. Pires. 2024. Bioenergetic trophic trade-offs determine mass-dependent extinction thresholds across the cenozoic. arXiv preprint arXiv:2410.18849 .

Yeakel, J. D., C. P. Kempes, and S. Redner. 2018. Dynamics of starvation and recovery predict extinction risk and both Damuth's law and Cope's rule. Nat. Comm. 9:1–10.